ISSN 1330-3651 (Print), ISSN 1848-6339 (Online)
https://doi.org/10.17559/TV-20201121231036
Original scientific paper

A Novel Ambiently Adaptive Atmospheric Water Generator Using Maximum Production Tracking Algorithm

Amin Danial ASHAM*, Wahied G. Ali ABDELAAL, Wael M. MAMDOUH

Abstract: In this paper, a Thermo-Electric Cooler (TEC) based ambiently adaptive Atmospheric Water Generator (AWG) system is proposed. Due to the advantages of TEC technology, it has been relied upon in the phase of dehumidifying the air flowing in the proposed system as an alternative to other mechanical methods. An AWG cooling control system has been developed based on the proposed algorithm to determine the temperature that achieves the highest productivity, which depends on the change in thermal load by changing the airflow, which keeps the temperature of the humid air inside the system below the Dew Point (DP) temperature at varying ambient conditions for sustainable water productivity. A novel Maximum Production Tracking (MPT) algorithm is introduced to automatically determine the marginal temperature below the DP for maximum productivity. The proposed system is simulated using MATLAB/SIMULINK under different ambient conditions. The obtained results affirmed the potential and verification of the proposed approach.

Keywords: atmospheric water generator (AWG); control; maximum production tracking (MPT); thermoelectric cooler (TEC)

1 INTRODUCTION

The availability of clean drinking water is a big challenge all over the Globe, especially with the huge rate of population growth and climate change. Nowadays, rivers and groundwater are becoming insufficient resources for drinking water. On the other hand, seawater is a sustainable source of water [1]. However, seawater requires costly desalination stations. This solution is not suitable for poor, developing countries and arid areas. AWG is an alternative and cost-effective solution adopted by many companies. This machine collects water vapor from humid air and treats it chemically to be healthy drinking water according to WHO standards. The idea is simple and based on the dehumidification of the atmospheric air. As shown in Fig. 1, the moist air is filtered to remove out dust and any other contaminating particles. Then the moist air is dehumidified to collect the water. At last, the collected water is treated by getting rid of bacteria and adding healthy salts.

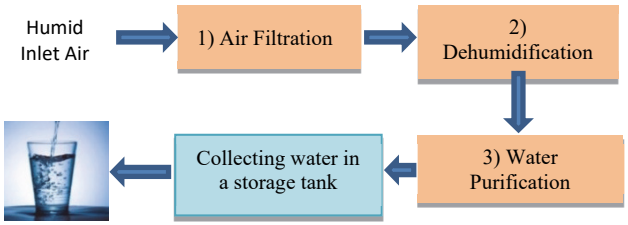

Figure 1 AWG processes

In the literature, different techniques are used for dehumidifying the moist air. The most common technologies used are refrigeration, air compression, and chemical desiccant-based systems. Refrigeration systems are based on heat pumps to cool down the moist air below the DP. Heat pumps could be mechanical, which are based on compressors and refrigerants. Such systems are used in Freon-based air conditioners. TEC modules are solid-state heat pumps, which have no moving parts. On the other hand, air compression technology extracts the water by compressing the moist air. Both mechanical (mechanical refrigeration and air compression) and chemical desiccant systems can produce up to several hundreds or thousands of liters per day. However, these systems are bulky systems with many moving parts and noise. They may be suitable as isolated water generation stations, not as portable compact machines for indoor applications.

Nowadays, TEC technology has a wide range of applications in several fields. This technology has several advantages over the mechanical refrigerator. TEC is smaller, lighter, quieter, and more reliable than mechanical cooling systems using compressors. The heat is pumped from the cold side of TEC to the hot side by the current flowing across the TEC module. This phenomenon is called the Peltier effect. TEC-based AWG machines are the most suitable for office and home applications because of their portability and quietness. Moreover, they can easily be powered directly from solar energy since TEC is a DC solid-state device. In this research, the TEC-based AWG system is proposed, which has a controlled airflow according to the ambient conditions (temperature and relative humidity) for keeping as sustainable productivity as possible. The proposed controller is targeting the produced water quantity by keeping the cooling air temperature below the dew point.

In [2, 3], a SPICE compatible equivalent circuit was developed for TEC and *Thermo-Electric Generator* (TEG). This model was useful for finding the small-signal transfer functions for designing feedback systems. An improved SPICE model of TEG was developed in [4]. This improved model included the temperature variations of the intrinsic internal parameters and the internal parasitic elements. A MATLAB-SIMULINK model of the thermoelectric module was developed in [5], which gives a friendly tool for simulation and control design. In [6], the thermal properties of TEC modules were investigated under different operating conditions. In [7], experimental research on using TEC technology for cooling electronic devices was conducted. In [8], an investigation was conducted to improve the Coefficient Of Performance (COP) of TEC modules. It was found that the multistage TEC configuration improves the COP of the system. However, multistage TEC modules are considerably more expensive than single TEC modules. In [9], a TEC-based AWG system was presented. This system was powered by solar cells. The experimental results of the system were

introduced. An optimized AWG system was designed using *Computational Fluid Dynamics* (CFD) in [10]. This system was designed considering many parameters such as temperature, humidity, airflow, and pressure. A study of the optimum number of TEC modules and the length of the condensation channel was presented in [11]. In both [12], [13], ON/OFF control systems were developed for dehumidifier systems. A dehumidifier system for the greenhouse application was introduced in [12], where a smartphone application was used to remotely monitor and manage the controlling module and sensor data of the dehumidifier, whereas a dehumidifier for *Ring Main Unit* (RMU) was developed in [13]. This dehumidifier system is powered by a solar system. The component of the system was optimized using Genetic algorithms.

In the literature, no AWG control system based on a maximum production algorithm was developed for maximum sustained productivity. In this article, a control system based on an MPT algorithm is proposed to automatically vary the airflow such that the temperature of the cooled air is always below the DP with an adaptive margin according to varying ambient conditions (temperature and relative humidity). The algorithm depends on measuring the temperature and relative humidity of the air, from which it is possible to calculate the specific humidity. The harvesting rate of water can be estimated from the specific humidity at the inlet and the outlet of the system and the airflow. As the airflow changes, the temperature changes and thus the amount of produced water. Therefore, the airflow that achieves the highest productivity must be maintained. In the next section, a mathematical analysis is introduced. Consequently, a complete control system is designed to control the airflow rate into the AWG system. Then a complete MATLAB-SIMULINK model is built to verify the performance of the proposed control system under different cooling capacities and ambient conditions.

2 MATHEMATICAL ANALYSIS

The system under consideration for the AWG application consists of a condensation pipe cooled with TEC modules. The entering humid air to the pipe will be cooled below the dew point temperature (DP) as depicted in Fig. 2.

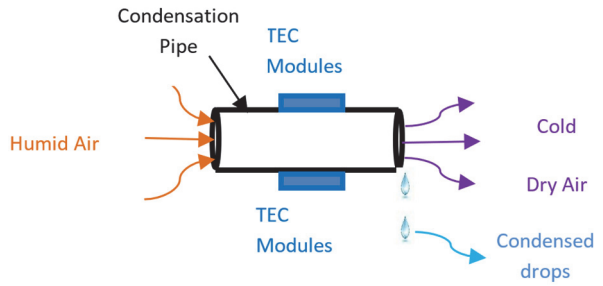

Figure 2 AWG system

At a steady-state, the humid air enters the condensation pipe at the ambient temperature T_a with a mass flow rate in kg/s. The thermal energy stored inside the condensation pipe is at a steady-state value. The cooled air exits from the pipe at a temperature T_o. The humid air is cooled from T_a to T_o where the heat is absorbed from the pipe by the TEC modules at the rate Q_c in Watts. From energy balance, we get [14]

$$Q_c = \dot{m}_a \left(h_a - h_o\right) - \dot{m}_w h_w \tag{1}$$

In Eq. (1), $\dot{m}_a$ and $\dot{m}_w$ are the dry air mass flow (kg/s) and condensation rate in (kg/s), respectively. Whereas, h_a, h_o and h_w are the enthalpies (kJ/kg dry air) of moist air at the inlet and outlet of the condensation pipe and the enthalpy of the condensed water at T_o, respectively [14]. Since the dry air and water vapor are considered ideal gases at pressure 1 atm and a temperature range from –10 °C to 50 °C, the mixture is also an ideal gas [14]. The enthalpy of moist air can be defined as $h = h_d + \omega h_v$, where h, h_d and h_v are the enthalpies of moist air, dry air, and water vapor at a certain temperature, respectively [14]. Whereas, ω is the specific humidity, which equals kg water vapor/kg dry air [14]. The enthalpy of dry air is approximated with $h_d = c_d T$ and c_d = 1.005 kJ/kg·°C [14]. The enthalpy of water vapor is approximated with $h_v = h_{vo} + c_v T$, where h_{vo} = 2500.9 kJ/kg and c_v = 1.82 kJ/kg·°C [14]. In addition, since the typical condensation rate in low power systems such as TEC based systems is very small, the second term of the right-hand side of Eq. (1) has a typical very low value compared to the first term and hence can be neglected. Hence, Eq. (1) can be rearranged to be as follows:

$$Q_c = \dot{m}_a \left[c_d (T_a - T_o) + h_{vo}\left(\omega_a - \omega_o\right) + c_v \left(\omega_a T_a - \omega_o T_o\right)\right] \tag{2}$$

where ω_a and ω_o are the specific humidity of the moist air at the inlet (ambient) and the outlet of the condensation pipe, respectively. In Eq. (2), for typical ambient conditions with a temperature range up to 35 °C with a relative humidity greater than 40% and T_o is less than the DP up to 10 °C, the values of the specific humidity are low enough to consider $c_v \left(\omega_a T_a - \omega_o T_o\right)$ negligible compared to the others terms. The ambient temperature T_a is considered constant since it varies very slowly. The moist air at the outlet of the condensation pipe is saturated. Consequently, the specific humidity at the pipe outlet ω_o is that of the saturated moist air at the temperature T_o. From the psychrometric chart, the specific humidity of saturated moist air can be obtained for the temperature range from C to 35 °C at the pressure of 1 atm.

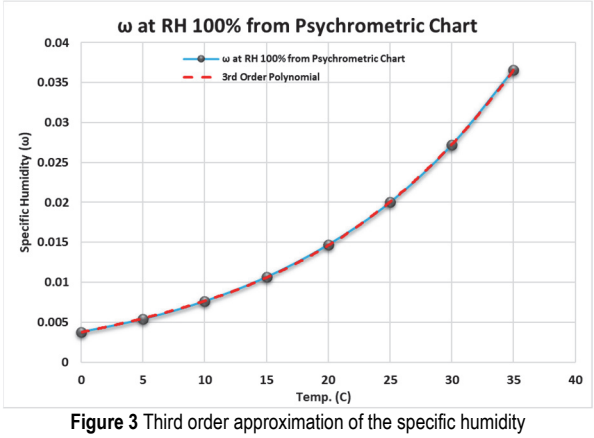

Figure 3 Third order approximation of the specific humidity

This data can be approximated using curve fitting by a third-order polynomial with high accuracy as shown in Fig. 3. As illustrated, the blue curve with black dots is drawn with the obtained data from the psychrometric chart at 1 atm. Whereas, the dashed red curve is the third-order curve fitting, which is $\omega = 4.46\times10^{-7}T^3 + 1.72\times10^{-6}T^2 + 3.32\times10^{-4}T + 3.72\times10^{-3}$. If T_o is changed around the current state a few degrees higher or lower, the relation between the specific humidity ω_o and temperature T_o can be considered linear. That is,

$$\omega_o = \eta + \lambda T_o \tag{3}$$

where η and λ can be obtained from the tangent line of the curve of ω_o from the psychrometric chart at the current temperature T_o. If we use Taylor's series of the third-order polynomial at a certain temperature, the first two terms represent the tangent at this temperature. This tangent is the linearization of the specific humidity with respect to temperature. In Fig. 4, the blue curve is the third-order polynomial, and the red dashed line is the tangent at $T = 15$ °C. The tangent parameters are $\eta = 0.0106$ and $\lambda = 0.0007$. As shown, the error between the tangent and the curve is less than 3% throughout 6 degrees.

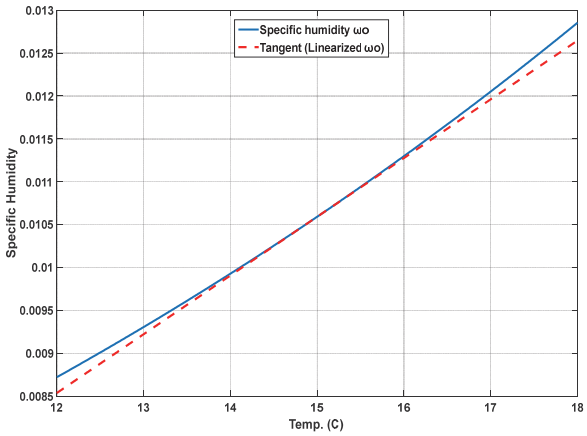

Figure 4 The blue curve is the specific humidity, and the orange line is the tangent at $T = 15$ °C

Therefore, it is justified to approximate the specific humidity at the outlet of the condensation pipe by a linear relation. From Eq. (2) and Eq. (3), we get:

$$Q_c = \dot{m}_a\left(c_d T_a + h_{vo}\left(\omega_a - \eta\right) - \left(c_d + h_{vo}\lambda\right)T_o\right) \tag{3}$$

Since $\dot{m}_a = \rho_a \Phi$, where ρ_a is the density of the dry air at the ambient temperature and Φ is the volumetric flow rate of the fan (m^3/s), Eq. (4) can be rearranged to be as follows:

$$Q_c = \rho_a \Phi \psi \delta T + \rho_a \Phi \gamma \tag{5}$$

where $\delta T = T_a - T_o$, $\psi = \left(c_d + h_{vo}\lambda\right)$ and $\gamma = h_{vo}\left(\omega_a - \eta - \lambda T_a\right)$. By solving for T_o from Eq. (5), we get:

$$T_o = T_a + \frac{\gamma}{\psi} - \frac{Q_c}{\rho_a \Phi \psi} \tag{6}$$

We can see from Eq. (6) that T_o can be decreased by increasing the cooling power Q_c or decreasing the air flow rate Φ. If it is desired to achieve a certain T_o with the maximum flow rate, the cooling power should be kept at its maximum value. In the AWG, the controller must keep the cooled air at a temperature below the DP. At the same time, the airflow should be high to get as much humid air as possible cooled and hence a larger amount of water can be harvested. Therefore, the controller may apply the maximum voltage to the TEC modules and change the T_o to be below the DP with a certain margin by changing the flow rate. However, as it will be shown later the cooling rate Q_c achieved by TEC modules depends on the temperature T_o.

If the controller changes the flow rate from Φ to $\Phi - \varphi$, then the temperature at the outlet changes from T_o to $T_o - t_o$ and the cooling rate becomes $Q_c + q_c$. The change in the cooling power q_c can be considered as the summation of two parts; the first part is responsible for a temperature change of the flowing air, which can be found from Eq. (5): $\left(\Phi - \varphi\right)\rho_a \psi t_o - \varphi\rho_a\left(\psi\delta T + \gamma\right)$, whereas the second part is needed to change the stored thermal energy in the system: $C\frac{dt_o}{dt}$, where C is the heat capacity of the condensation pipe system, which can be considered constant for a small temperature variation. The total change in the cooling rate q_c is expressed in Eq. (7).

$$q_c = \left(\Phi - \varphi\right)\rho_a c_d t_o - \varphi\rho_a\left(c_d\delta T + \gamma\right) + C\frac{dt_o}{dt} \tag{7}$$

$$C\frac{dt_o}{dt} + \left(\Phi - \varphi\right)\rho_a c_d t_o = q_c + \varphi\rho_a\left(c_d\delta T + \gamma\right) \tag{8}$$

Therefore,
as shown in Eq. (8), the system is first order. However, since the flow rate can be altered, the system is time-variant. The cooling power q_c will be got from the mathematical model of the TEC module. From [6, 7, 15], the heat flow through the cold side Q_c, hot side Q_h and the voltage V applied to the TEC module is given as follows:

$$Q_c = \alpha I T_c - k\Delta T - \frac{1}{2}I^2 R \tag{9}$$

$$Q_h = \alpha I T_h - k\Delta T + \frac{1}{2}I^2 R \tag{10}$$

$$V = \alpha\Delta T + IR \tag{11}$$

where α, k, I and R are the Seebeck coefficient (V/K), the thermal conductance (W/K), the electrical current (A), and the electrical resistance (Ohms) of the TEC module, respectively. Whereas T_h, T_c and ΔT are the temperature of

the hot side, cold side, and the temperature difference ($T_h - T_c$) of the TEC module, respectively. The ambient temperature T_a and the temperature of the cooled air T_o are related to the hot side T_h and cold side T_c temperatures, as shown in Eq. (12) and Eq. (13).

$$T_a = T_h - Q_h r_h \tag{12}$$

$$T_o = T_c + Q_c r_c \tag{13}$$

where the r_h and r_c are the thermal resistances connected to the hot side and cold side of the TEC module, respectively. From Eq. (9) to Eq. (13), we can get an expression of Q_c as shown in Eq. (14).

$$Q_c = \frac{2I\alpha T_o - 2VIkr_h - 2k\delta T - I^2R}{2\left(1 + I\alpha r_c + k(r_c + r_h)\right)} \tag{14}$$

For a typical TEC module with 127 thermo-electrical element pairs: α = 0.0508 V/K, k ranges from 0.9 to 0.14 W/K [16]. If r_c is sufficiently small the term $I\alpha r_c$ can be ignored and hence the denominator of the right-hand side of Eq. (14) does not depend on the electrical current. Moreover, the power is usually supplied to the TEC module using a voltage ource and hence V is constant. From Eq. (11), in case of constant voltage V the current I will change as the ΔT changes. However, ΔT does not change widely and hence the current change is small enough to be considered constant. Under these conditions, Eq. (14) comes in the following form:

$$Q_c = aT_o + b \tag{15}$$

where a and b are constants, which are functions of the thermal resistances, electrical current, and voltage and ambient temperature. Consequently, Q_c is linearly dependent on T_o. From Eq. (15), if T_o changes to $T_o - t_o$, then Q_c changes to $Q_c + q_c$ and hence q_c is as in Eq. (16).

$$q_c = -at_o \tag{16}$$

Substituting from Eq. (16) into Eq. (8), we get:

$$C\frac{dt_o}{dt} + \left(\Phi - \varphi\right)\rho_a c_d t_o = -at_o + \varphi\rho_a\left(c_d\delta T + \gamma\right) \tag{17}$$

Therefore,

$$C\frac{dt_o}{dt} + \left(\left(\Phi - \varphi\right)\rho_a c_d + a\right)t_o = \varphi\rho_a\left(c_d\delta T + \gamma\right) \tag{18}$$

From Eq. (18), if the volumetric flow rate is small enough and the number of TEC modules used is sufficient such that $\left(\Phi - \varphi\right)\rho_a c_d$ is ignored compared to a, which can be increased by increasing the number of TEC modules. Therefore Eq. (18) becomes:

$$C\frac{dt_o}{dt} + at_o = \varphi\rho_a\left(c_d\delta T + \gamma\right) \tag{19}$$

The system approximated by Eq. (19) is a Linear Time-Invariant (LTI) first-order system of type 0. Therefore, a PI controller can be used to keep the temperature of the cooled air to be less than the DP and hence the condensation takes place even when the ambient conditions change. In the following section, a control scheme of an adaptive AWG system using the proposed MPT algorithm is introduced. This control scheme changes the air flow rate to keep the temperature below the DP with varying margin based on the ambient conditions.

3 AMBIENTLY ADAPTIVE AWG SYSTEM

3.1 Control Scheme

As shown in the previous section, the dynamics of an AWG can be approximated by a linear first-order system of type zero. In real life, the ambient conditions are not fixed and hence the *DP* varies with time during the day and the night. Also, the AWG system may have some malfunctions with cooling elements affecting the cooling capacity. Consequently, for sustainable water condensation, the humid air must be always cooled to a temperature below the *DP*.

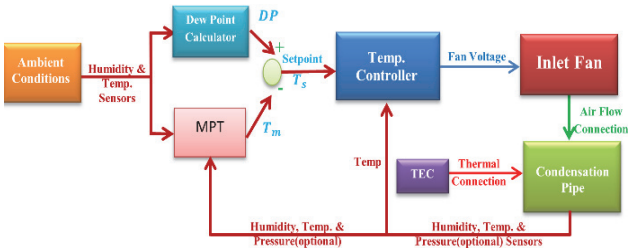

Figure 5 Adaptive AWG system

In Fig. 5 a control scheme is proposed to cool down the humid air to a temperature $T_s < DP$ by changing the flow rate of the air pushed into the system. Since the dynamics of the system can be viewed as an LTI system of type zero, therefore a PI $(k_p e + k_i \int e dt)$ (temperature controller) isused. The error e is the difference between the set point T_s and the actual temperature of the cooled air. Whereas k_p and k_i are the gains of the proportional and integral parts, respectively. The question here is how to determine the set point T_s. The set point T_s is chosen to be less than the *DP* by a marginal value T_m as in Eq. (20). The marginal temperature T_m is obtained by the proposed MPT algorithm.

$$T_s = DP - T_m \tag{20}$$

Noting that, the water condensation rate (g/s) at the steady-state can be approximated by $\dot{m}_a \times \left(\omega_a - \omega_o\right) = \Phi\rho_a \times \left(\omega_a - \omega_o\right)$ assuming the pressure is constant where, ρ_a is the density of the dry air at the ambient temperature. The term $\left(\omega_a - \omega_o\right)$ represents the condensed water per the unit mass of dry air. In case of a high flow rate, the air will not be cooled enough, and hence the term $\left(\omega_a - \omega_o\right)$ will be smaller and hence decreasing

the condensation rate. On the other hand, a very low airflow rate Φ will reduce the quantity of humid air pumped into the AWG system and consequently a low condensation rate.

In the case of increasing T_m the set point decreases and consequently the flow rate Φ decreases, whereas $(\omega_a - \omega_o)$ increases. On the other side, decreasing T_m leads to a higher setpoint and hence higher flow rate and lower $(\omega_a - \omega_o)$. At this point, the role of the introduced MPT algorithm begins. The MPT algorithm searches for the marginal temperature T_m that maximizes the quantity $\Phi\rho_a \times(\omega_a - \omega_o)$ and hence the water production is maximized. The density of the ambient dry air can be considered constant as the change of the temperature is very slow. Therefore, the MPT algorithm just maximizes $\Phi\times(\omega_a - \omega_o)$.

As illustrated in Fig. 5, the ambient conditions (ambient temperature T_a and relative humidity RH_a) and the temperature T_o and the relative humidity RH_o at the outlet of the condensation pipe are measured. The DP is calculated from T_a and RH_a using Magnus formula [17]. Whereas, ω_a (from T_a, RH_a and atmospheric pressure P_a) and ω_o (from T_o, RH_o and the pressure inside the condensation pipe P_o) are calculated using formulas in [14, 18].

3.2 Maximum Production Tracking Algorithm

The MPT algorithm searches for the marginal temperature T_m that gives the maximum water production. This algorithm uses the quantity $\Phi\times(\omega_a - \omega_o)$ as a production index Idx. Therefore, the main objective of the MPT algorithm is to maximize $\Phi\times(\omega_a - \omega_o)$. The algorithm steps are as follows:

1. Initialization:
   a. $T_m = \sigma_{min}$ (the minimum allowed value).
   b. $stp = 1$ (T_m is incremented or decremented by steps stp)
   c. Calculate $\Phi\times(\omega_a - \omega_o)$, then let $Idx = \Phi\times(\omega_a - \omega_o)$
   d. $\theta = 1$ (a certain factor used to suppress the update of T_m)
2. $\Delta\omega_a = \left|(\omega_a - \omega_{-1})\right|$
3. $\omega_{-1} = \omega_a$
4. The DP is calculated and consequently the set point T_s is obtained from Eq. (20).
5. The setpoint is applied to the temperature controller (PI controller).
6. If the temperature error $e = T_s - T_o < \varepsilon$ ($\varepsilon = 0.1$ °C) for a period longer than a certain time t_{ss} (t_{ss} = 60 s) an indication of the steady-state situation, then $\Phi\times(\omega_a - \omega_o)$ is calculated.
   a. If $(\Delta\omega_a \geq \varepsilon\times(\omega_a - \omega_o))$, then $\theta = 0$ (to guarantee that no productivity check while the ambient humidity changes widely)
   else
      i. $\theta = 1$
      ii. If the $\Phi\times(\omega_a - \omega_o) > Idx$ (previous value), then
         1) $stp = \mu_{inc} \times stp.$
         2) If $|stp| > v_{max}$, then $stp = sign(stp)\times v_{max}$.
      iii. If the $\Phi\times(\omega_a - \omega_o) > Idx$ (previous value), then
         1) $stp = -\mu_{dec} \times stp$.
         2) If $|stp| < v_{min}$, then $stp = sign(stp)\times v_{min}$.
   b. The marginal temperature is updated:
      i. $T_m = T_m + \theta \times stp$
      ii. If $T_m > \sigma_{max}$, then $T_m = \sigma_{max}$
      iii. If $T_m < \sigma_{min}$, then $T_m = \sigma_{min}$
   c. $Idx = \Phi\times(\omega_a - \omega_o)$
7. Go to step 2.

where v_{max}, v_{min}, σ_{max}, σ_{min}, μ_{inc}, μ_{dec}, and ε are the maximum step value, minimum step value, maximum allowed value for T_m, the minimum allowed value for T_m, step increment factor, step decrement factor, and the maximum allowed ratio of $\Delta\omega_a$ to $(\omega_a - \omega_o)$, respectively.

In the following section, a Simulink model of an AWG system with the proposed ambiently adaptive control scheme using the MPT algorithm is built. The controller performance under different conditions is demonstrated.

4 AWG MATLAB-SIMULINK MODEL

In this section, a dynamic model of a TEC-based AWG is built using SIMULINK. The complete model with the proposed control scheme is shown in Fig. 6.

4.1 The Complete Model Consists of Four Main Subsystems

a) The environmental data subsystem generates the *ambient temperature* (T_a) and the *ambient relative humidity* (RH_a) in Cairo during the 24 hours of 12 days all over the year. Each day belongs to a month from October 2018 to September 2019

b) The measurements subsystem is for the scopes that display selected signals of the system such as applied voltage to TEC modules, drawn current by TEC modules COP, temperature and relative humidity inside the condensation pipe, ambient temperature, ambient relative humidity, condensation rate, total condensed water, and other relevant signals

c) The application subsystem consists of a condensation pipe with TEC modules and an electric fan. In Fig. 7, the complete model is illustrated. The cooling system is built using 6 TEC modules; each one has a maximum cooling power of 40 watts. TEC modules are represented in a single subsystem. The TEC modules are electrically parallel, and serial thermally. In the model, the cold and the hot surfaces of the TEC modules are represented by port A and port B, respectively.

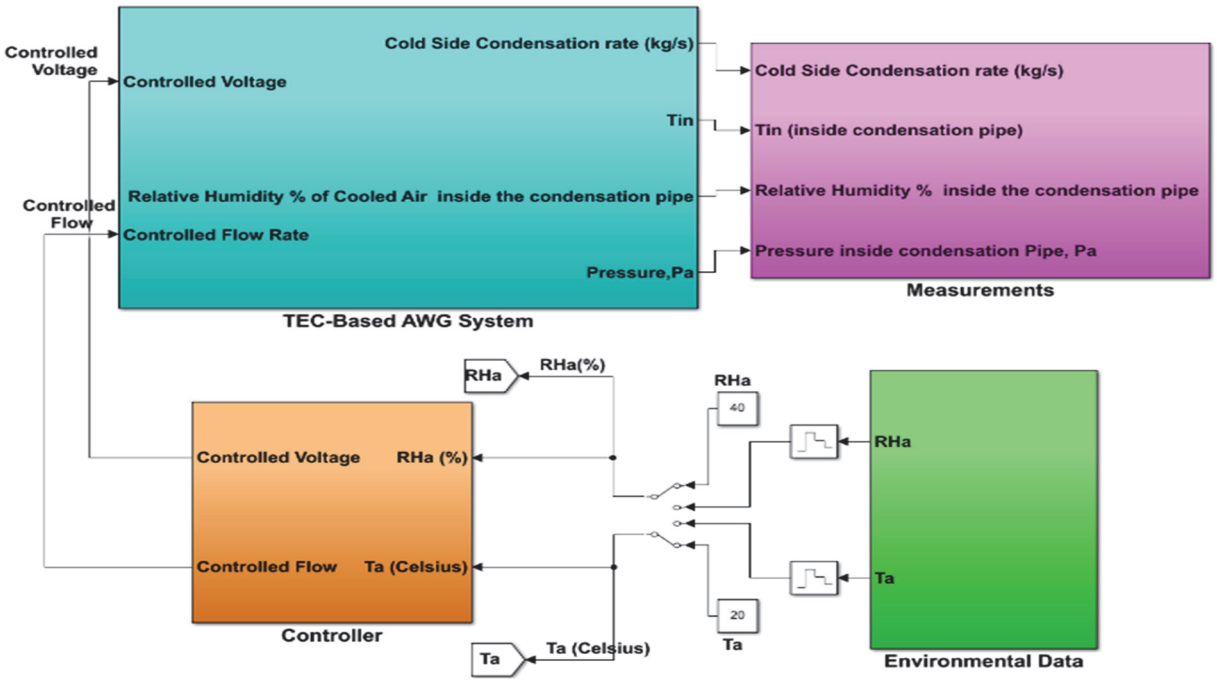

Figure 6 TEC based AWG dynamical SIMULINK model

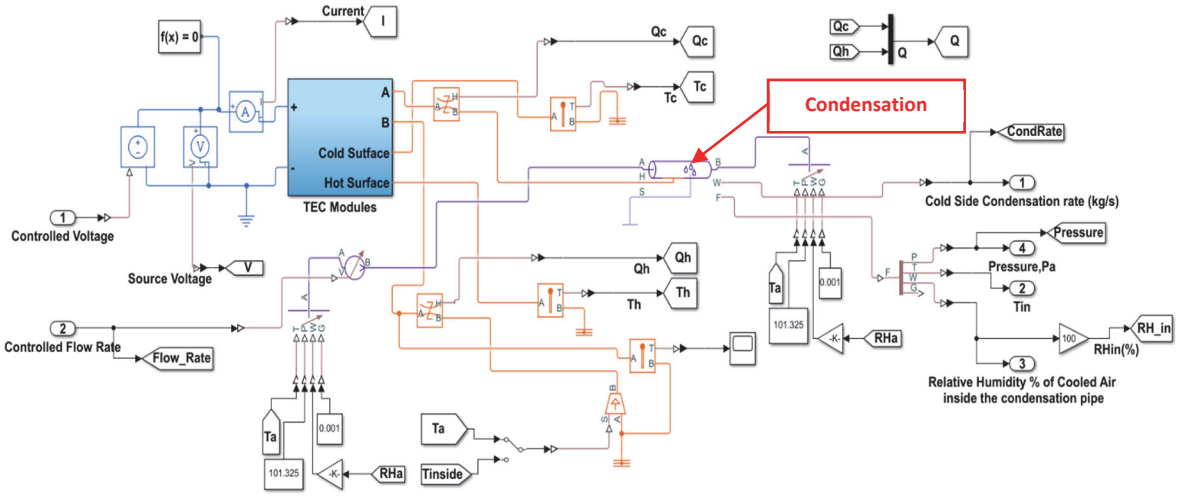

Figure 7 Complete TEC-based AWG model

Port A is connected to the condensation pipe through the thermal resistance, which represents the thermal path from the cooling pipe walls to the cold side of the TEC module. Port B is connected to the ambient air through the thermal resistance of the hot surface fins. The relations between the absorbed heat on the cold side, the emitted heat from the hot side, the temperature difference between cold and hot sides, injected current, and the applied voltage are described by Eq. (9) to Eq. (11). The moist air is fed into the condensation pipe as illustrated in Fig. 7, via a controlled volumetric flow rate source. The ambient conditions can be changed by varying the reservoir parameter during the simulation, where the parameters are fed from the external signals into the reservoir. More details about the elements used in this model can be found in [19].

d) The controller subsystem adapts the operation of the AWG to ensure that the condensation takes place in all conditions if possible. This controller measures the ambient conditions (T_a and RH_a) and calculates the corresponding dewpoint. The MPT algorithm searches for a marginal temperature T_m, which produces the maximum productivity. Based on the calculated dewpoint and the marginal temperature a setpoint for the temperature inside the condensation is generated. The temperature at the outlet of the condensation pipe is measured as feedback and hence the flow rate is adjusted using a PI controller to achieve the required temperature setpoint as shown in Fig. 8.

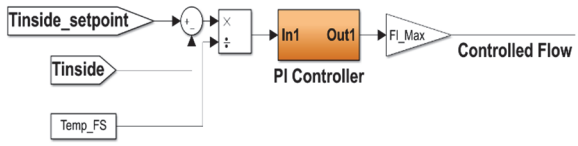

Figure 8 Temperature controller (changes flow rate)

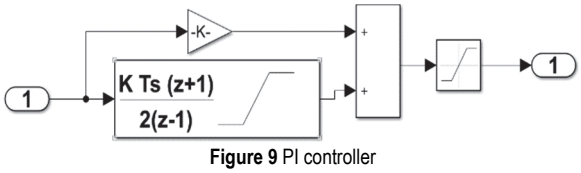

Figure 9 PI controller

The PI controller is illustrated in Fig. 9. And the MPT algorithm is implemented using a MATLAB function block as depicted in Fig. 10.

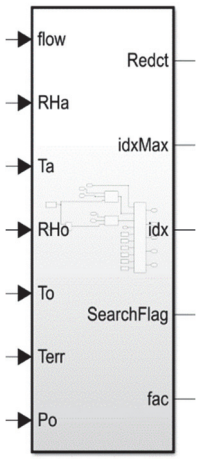

Figure 10 MPT algorithm

4.2 Simulation Results

The complete model of AWG is simulated to demonstrate the performance of the proposed control scheme. The AWG simulated here has a condensation pipe with a length of 1 m and a diameter of 1 cm. The parameters of the model are listed hereafter. The detailed descriptions of the Simulink blocks are in [19, 20] :

- $k_p = 1,\ k_i = 0.01, v_{max} = 1, v_{min} = 0.1, \sigma_{max} = 9, \sigma_{min} = 1,$ $\mu_{inc} = 1.1, \mu_{dec} = 0.5$ and $\varepsilon = 0.01$.
- Number of TEC modules = 6
- $S = 200\ e^{-6}$ V/K (Seebeck coefficient)
- ρ = $10e^{-6}$ Ω·m (electrical resistivity of the TEC elements)
- k = 1.5 W/K·m (Thermal conductivity of the TEC elements)
- TEC module resistance = 2 Ω
- Number of pairs of thermoelectric elements in each TEC module = 127
- Cold side Thermal Resistance = 0.1 K/W
- Hot side Thermal Resistance = 0.4 K/W
- Pipe Length = 1 m
- Pipe diameter = Hydraulic Diameter = 0.01 m
- Cross Section Area = $\frac{\pi(\text{Pipe diameter})^2}{4}$ m^2
- Aggregate equivalent length = 0.1 m
- Internal surface absolute roughness = $15e^{-6}$ m
- Laminar flow upper Reynolds number limit = 2000
- Turbulent flow lower Reynolds number limit = 4000
- Shape factor for laminar flow viscous friction = 64
- Nusselt number for laminar flow heat transfer = 3.66

The TEC modules are powered by a voltage source, which applies a fixed voltage of 12 V. To demonstrate the performance and importance of the MPT algorithm, the AWG is simulated for three relative humidity values (40%, 60%, 80%) at ambient temperature 32 °C. In Tab. 1, the simulation results of 6 TECs-AWG are listed. At every relative humidity, the productivity per day is recorded for different fixed values of T_m without the MPT algorithm. Then the productivity using the MPT algorithm is tabulated. The MPT algorithm is used twice; first when the measured pressure inside the condensation pipe $(meas.P_o)$ is used to calculate ω_o and second, assuming the pressure does not change, that is $P_o = P_a$, where P_a is the ambient pressure (101.325 kPa).

Tab. 2 presents the same data as Tab. 1 except that only 4 TEC modules are used instead of 6 TEC modules.

As illustrated in Tab. 1 and Tab. 2 the water production depends on the marginal temperature T_m. The value of T_m of the maximum productivity depends on the ambient conditions and the cooling capacity.

Table 1 Water productivity of 1m condensation pipe cooled with 6 TEC modules

T_m	Water Productivity (cm^3/day) (water density = 1 g/cm^3 T_a = 32 °C		
	RH_a = 40%	RH_a = 60%	RH_a = 80%
1	366.4	790.9	1348
2	529.5	1063	1719
3	621.5	1206	1887
4	660.4	1252	1891
5	661.6	1221	1779
6	637.4	1140	1604
MPT $(meas.P_o)$	660.5	1245	1895
MPT $(P_o = P_a)$	660	1244	1881

Table 2 Water productivity of 1m condensation pipe cooled with 4 TEC modules

T_m	Water Productivity (cm^3/day) (water density = 1 g/cm^3 T_a = 32 °C		
	RH_a = 40%	RH_a = 60%	RH_a = 80%
1	256	572	1011
2	377	780	1300
3	442	876	1401
4	468	899	1373
5	469	870	1274
6	453	811	1144
MPT $(meas.P_o)$	469	894	1398
MPT $(P_o = P_a)$	468	895	1388

Without the MPT algorithm, T_m of the maximum production can be determined for certain ambient conditions and cooling capacity. However, in the case of losing cooling capacity (a faulty TEC module) or variations of ambient conditions, T_m of the maximum production needs to be updated with a new value. The MPT algorithm continuously searches for T_m that corresponds to the maximum water harvesting in the current situation.

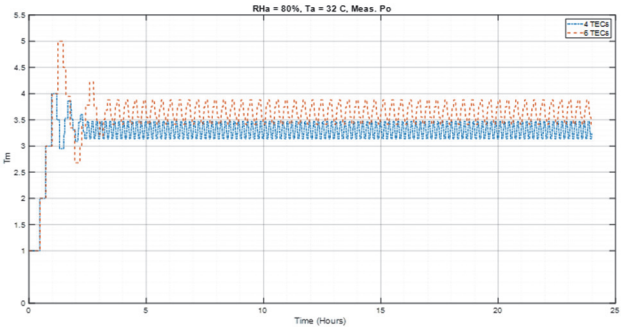

Figure 11 Generated marginal temperature T_m by MPT algorithm

Fig. 11 shows the marginal temperature T_m generated by the MPT algorithm. In the case of 6 TEC modules the temperature swings between 3.42 °C and 3.88 °C, where

the optimum value is about 3.5 °C which gives the productivity of 1907 cm^3/day. On the other hand, in the case of 4 TEC modules the temperature swings between 3.14 °C and 3.47 °C and the highest productivity 1403 cm^3/day occurs at $T_m = 3.2$ °C.

The MPT was able to track the best value of T_m for maximum water production. To assess the performance of the MPT algorithm, the efficiency of water production at current conditions is defined as follows:

$$Production\ Efficiency = \\ = \frac{Production\ using\ the\ MPT\ algorithm}{Maximum\ Production\ using\ the\ best\ fixed\ T_m} \quad (21)$$

Using Eq. (21), the efficiency of the MPT algorithm is greater than 98%. Besides, the MPT algorithm adapts the highest productivity in case of varying conditions.

The MPT algorithm is tested using a variable ambient humidity and temperature. The weather data of Cairo on the 1st of July 2019 is used [21]. In Fig. 12, the ambient relative humidity and the ambient temperature are depicted. As shown the ambient conditions vary with time.

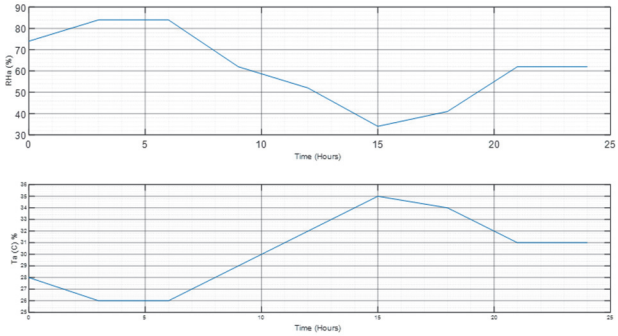

Figure 12 Ambient humidity RH_a and temperature T_a of 1st July 2019

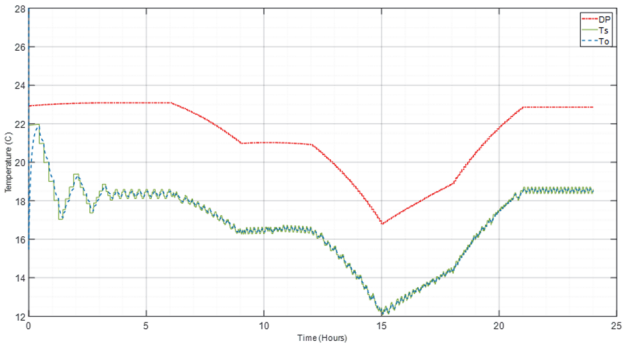

Figure 13 Dew Point, set point T_s, and the outlet temperature T_o

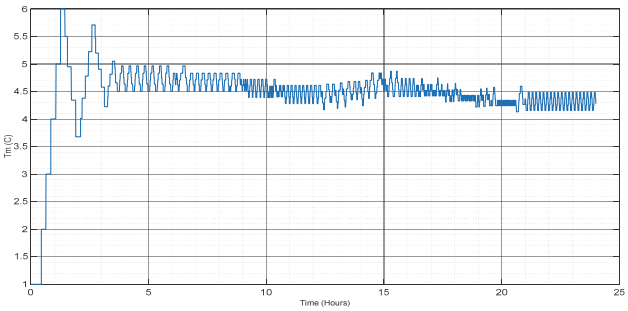

Figure 14 The marginal temperature T_m generated by the MPT algorithm

The calculated dew point is depicted in Fig. 13. The dew point changes with ambient humidity and temperature. The setpoint is below the dew point by the marginal temperature T_m as illustrated in Fig. 13. The flow controller controls the actual outlet temperature T_o to follow the setpoint as manifested in Fig. 13. Therefore, sustainable water condensation is achieved since the setpoint is always below the dew point. The marginal temperature generated by the MPT algorithm is illustrated in Fig. 14.

Table 3 Water Production Comparison of 1st July 2019 using 6 TEC modules

	MPT	T_m = 1 °C	T_m = 2 °C	T_m = 3 °C	T_m = 4 °C	T_m = 5 °C	T_m = 6 °C
Water Production / cm^3/day	1210	741	1008	1161	1222	1207	1143

In Tab. 3, the water production of the MPT algorithm and for different fixed values of T_m is tabulated. The MPT algorithm was able to produce 99% of the maximum production. Since the algorithm takes time to find the best T_m, therefore, its efficiency is less than 100%. The fixed marginal temperature corresponding to maximum productivity must be determined manually for the current cooling capacity and ambient conditions. On the other hand, the MPT algorithm searches for it automatically. Moreover, in the case of severe changes such as deficiency of the cooling system, the MPT algorithm will automatically search for the most suitable new T_m for maximum productivity.

5 CONCLUSION

In this research, mathematical analysis was conducted, which shows that an AWG system based on thermoelectric modules can be approximated by a first-order LTI model. A control scheme based on the proposed maximum production tracking MPT algorithm was developed to achieve two main goals: first, to ensure sustainable water production even with variable ambient conditions by keeping the humid air cooled below the *DP*. Second, the operating point is kept close to the optimal point for maximum production even in case of partial cooling deficiency. It was shown that the value of the marginal temperature T_m affects productivity. The proposed MPT algorithm continually searches for the best T_m that corresponds to maximum productivity. A definition of production efficiency was introduced, as shown in Eq. (21), to evaluate the performance of the proposed MPT algorithm. The production efficiency of the MPT algorithm was greater than 98% in all the conducted simulations.

The MPT algorithm can be used even with refrigerant-based AWG systems to seek optimal airflow for the highest water productivity.

Our future work will focus on integrating the TEC technology and the proposed MPT algorithm-based control scheme with an optimized mechanical design to maximize productivity while meeting the portability and quietness required for home and office applications.

Acknowledgments

The authors would like to thank the Academy of Scientific Research and Technology (ASRT), Cairo -Egypt for the financial support provided to the research project

"Design and Implementation of Atmospheric Water Generator" under the framework of the initiatives program.

6 REFERENCES

[1] *Water | United Nations*. (n.d.). Retrieved August 30, 2020, from https://www.un.org/en/sections/issues-depth/water/

[2] Lineykin, S. & Ben-Yaakov, S. (2005). Analysis of thermoelectric coolers by a spice-compatible equivalent-circuit model. *IEEE Power Electronics Letters*, *3*(2), 63-66. https://doi.org/10.1109/LPEL.2005.846822

[3] Lineykin, S. & Ben-Yaakov, S. (2007). Modeling and analysis of thermoelectric modules. *IEEE Transactions on Industry Applications*, *43*(2), 505-512. https://doi.org/10.1109/TIA.2006.889813

[4] Moumouni, Y. & Jacob Baker, R. (2015). Improved SPICE modeling and analysis of a thermoelectric module. *Midwest Symposium on Circuits and Systems*, *2015-September*. https://doi.org/10.1109/MWSCAS.2015.7282015

[5] Tsai, H. L. & Lin, J. M. (2010). Model building and simulation of thermoelectric module using Matlab/Simulink. *Journal of Electronic Materials*, *39*(9). https://doi.org/10.1007/s11664-009-0994-x

[6] Chang, Y.-W., Cheng, C.-H., Wu, W.-F., & Chen, S.-L. (2007). An Experimental Investigation of Thermoelectric Air-Cooling Module. *International Journal of Mechanical and Mechatronics Engineering*, *1*(9), 466-471.

[7] Sun, X., Yang, Y., Zhang, H., Si, H., Huang, L., Liao, S., & Gu, X. (2017). Experimental Research of a Thermoelectric Cooling System Integrated with Gravity Assistant Heat Pipe for Cooling Electronic Devices. *Energy Procedia*, *105*, 4909-4914. https://doi.org/10.1016/j.egypro.2017.03.975

[8] Patel, J., Patel, M., Patel, J., & Modi, H. (2016). Improvement in the COP Of Thermoelectric Cooler. *International Journal of Scientific & Technology Research*, *5*, 5.

[9] Nandy, A., Saha, S., Ganguly, S., & Chattopadhyay, S. (2014). A Project on Atmospheric Water Generator with the Concept of Peltier Effect. *International Journal of Advanced Computer Research*, *4*(15), 481.

[10] Suryaningsih, S. & Nurhilal, O. (2016). Optimal design of an atmospheric water generator (AWG) based on thermo-electric cooler (TEC) for drought in rural area. *AIP Conference Proceedings*, *1712*. https://doi.org/10.1063/1.4941874

[11] Eslami, M., Tajeddini, F., & Etaati, N. (2018). Thermal analysis and optimization of a system for water harvesting from humid air using thermoelectric coolers. *Energy Conversion and Management*, *174*, 417-429.

[12] Lee, Y. J., Park, K. W., & Kim, E. K. (2015). Automatic dehumidifier control system for greenhouse using smart phone. *Lecture Notes in Electrical Engineering*, *352*. https://doi.org/10.1007/978-3-662-47487-7_38

[13] Yang, Y., Ding, Y., Wang, Y., Gong, C., Chen, F., & Lv, L. (2019). Power Optimal Matching and Humidity Intelligent Control of Ring Main Unit Dehumidification System. *IECON Proceedings (Industrial Electronics Conference)*, *2019-October*. https://doi.org/10.1109/IECON.2019.8926779

[14] Cengel, Y. A. & Boles, M. A. (2015). *Thermodynamics: an Engineering Approach*. McGraw-Hill (8th ed.).

[15] Belovski, I., Staneva, L., Aleksandrov, A., & Rahnev, P. (2017). Mathematical Model of Thermoelectric Peltier Module. *Journal of Communication and Computer*, *14*(2).

[16] *TEC Modules | Q ATS*. (n.d.). Retrieved September 7, 2020, from https://www.qats.com/Products/TEC/TEC-Modules

[17] Lawrence, M. G. (2005). The relationship between relative humidity and the dewpoint temperature in moist air: A simple conversion and applications. *Bulletin of the American Meteorological Society*, *86*(2). https://doi.org/10.1175/BAMS-86-2-225

[18] Oyj, V. (2013). Humidity Conversion Formulas - Calculation formulas for humidity. *Humidity Conversion Formulas*.

[19] *Simscape Documentation*. (n.d.). Retrieved October 8, 2020, from https://www.mathworks.com/help/physmod/simscape/index.html

[20] *Rigid conduit for moist air flow - MATLAB*. (n.d.). Retrieved August 30, 2020, from https://www.mathworks.com/help/physmod/simscape/ref/pipema.html?s_tid=srchtitle.

[21] *Past Weather in Cairo, Egypt - Yesterday or Further Back*. (n.d.). Retrieved August 30, 2020, from https://www.timeanddate.com/weather/egypt/cairo/historic

Contact information:

Amin Danial ASHAM, PhD
(Corresponding author)
Egyptian Academy for Engineering and Advanced Technology,
Km 3 Cairo Belbeis Desert Rd, Cairo, Egypt
E-mail: amin.danial@eaeat.edu.eg

Weal M. MAMDOUH, PhD
Egyptian Academy for Engineering and Advanced Technology,
Km 3 Cairo Belbeis Desert Rd, Cairo, Egypt
E-mail: wael@eaeat.edu.eg

Wahied G. Ali ABDELAAL, PhD, Professor
Egyptian Academy for Engineering and Advanced Technology,
Km 3 Cairo Belbeis Desert Rd, Cairo, Egypt
E-mail: wahied@eaeat.edu.eg